

Tropical Atlantic sea level variability from Geosat (1985-1989)

S. Arnault*

Laboratoire d'Océanographie Dynamique et de Climatologie, Unité Mixte de Recherche 121 Centre National de Recherche Scientifique, Institut Français de Recherche Scientifique pour le Développement en Coopération (ORSTOM), Université Pierre et Marie Curie, Paris

R. E. Cheney

Satellite and Ocean Dynamics Branch, National Oceanic and Atmospheric Administration
Silver Spring, Maryland

O. R. S. T. O. M. Fonds Documentaire

N° : 42207

Cote : B Ex 1

Abstract. Geosat altimeter data between April 1985 and September 1989 are analyzed in the tropical Atlantic Ocean. First, improvements due to the use of new corrections and orbit computations are found to be effective, especially in the Gulf of Guinea, where part of the previously missing signal is recovered. Then, the variability of the ocean is examined using empirical orthogonal functions (EOFs). Only three EOFs are needed to describe 80% of the seasonal variance. The first one describes the meridional tilting of the tropical Atlantic along the mean location of the Intertropical Convergence Zone, with an annual period. The second describes a mass redistribution due to the equatorial upwelling peaking in June-July. The third function presents a clear semiannual signal. Looking at interannual variability, the first EOF reveals a mass redistribution between the equatorial region (10°N to 10°S) and the northern and southern ones (10°N to 30°N, 10°S to 30°S). In the equatorial region the upper layer volume increases from about -1.5 to $1.5 \times 10^{14} \text{ m}^3$ between 1987 and 1989. Occurring 1 year after the Pacific El Niño, this phenomenon recalls the 1984 anomaly observed during the Programme Français Océan et Climat en Atlantique Tropical/Seasonal Equatorial Atlantic experiments.

1. Introduction

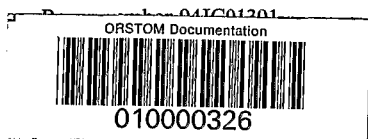
Tropical ocean dynamics are characterized by a two-layer system and a vanishing Coriolis parameter which results in a strong and rapid response of the ocean to the wind forcing. However, each of the tropical oceans (Indian, Pacific, Atlantic) is somewhat different. Recently, *Philander and Chao* [1991] pointed out the importance of the wind scales, especially of the spatial scales compared to the ocean width, to explain differences found between the Pacific and the Atlantic variability: the tropical Atlantic responds mostly on a seasonal time scale and in equilibrium with the wind forcing, contrary to the Pacific where interannual El Niño events and free wave propagation are dominant. However, during the 1982-1984 Programme Français Océan et Climat en Atlantique Tropical/Seasonal Equatorial Atlantic program (FOCAL/SEQUAL) originally planned to investigate the seasonal cycle in the tropical Atlantic, several studies based on high-quality data sets showed an interannual signal with the presence of abnormal warm waters in the Gulf of Guinea in early 1984 [*Houghton and Colin*, 1986; *Hisard and Hénin*, 1987; *Philander*, 1986] and free wave propagation along the equator in response to wind bursts [*Katz*, 1987; *Garzoli*, 1987].

A major experiment such as FOCAL/SEQUAL, combining hydrological cruises, moorings, inverted echo sounders, and tide gauges, is difficult to maintain over several years. Satellite altimetry offers one practical solution for obtaining

the long-term observations, though limited to surface topography. Seasat and Geosat altimeter data have been used extensively in the tropical regions; Kelvin and Rossby waves have been tracked along the equatorial Pacific during the 1986-1987 El Niño [*Miller et al.*, 1988; *Delcroix et al.*, 1991] as well as Legeckis waves [*Malarde et al.*, 1987; *Périgaud*, 1990]. In the Atlantic, altimetric data have been successfully compared with in situ data [*Ménard*, 1988; *Carton and Katz*, 1990; *Arnault et al.*, 1992a] or with model results [*Arnault et al.*, 1992b; *Diden and Schott*, 1992].

Recently, two new sets of Geosat data have been released by the National Oceanic and Atmospheric Administration (NOAA): crossover difference records (XDRs) from the geodetic mission [*Cheney et al.*, 1991a] and geophysical data records (GDRs) from the exact repeat mission [*Cheney et al.*, 1991b]. Both XDRs and GDRs contain a significantly improved water vapor correction derived from two satellite sensors operating during the Geosat mission: the TIROS operational vertical sounder (TOVS) and the special sensor microwave imager (SSM/I). Compared to the previously available water vapor field, obtained from the Fleet Numerical Oceanographic Center (FNOC), the TOVS/SSM/I correction contains more detailed spatial structures and variability, especially in the tropics, and constitutes a real improvement [*Zimbelman and Busalacchi*, 1990; *Emery et al.*, 1990]. In addition, the GDRs are based on the more accurate orbit computed by *Haines et al.* [1990] using the Goddard Earth Model (GEM) T2 geopotential model of *Marsh et al.* [1990]. This orbit has a precision of approximately 40 cm, an improvement of nearly a factor of 10 compared to the original Geosat GDRs.

Copyright 1994 by the American Geophysical Union.



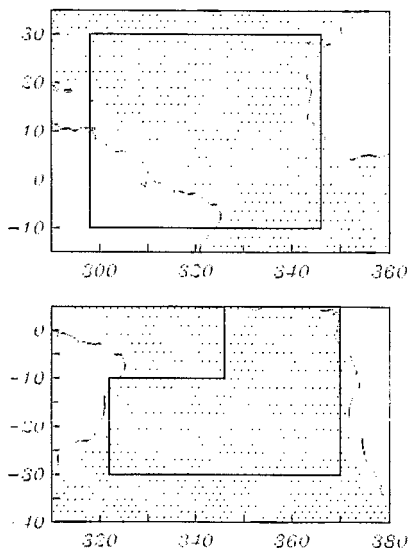


Figure 1. Regions over which the Geosat analysis was performed. The data were processed separately in northern and southern regions in an attempt to obtain relatively long arcs of uniform length. Orbit errors were modeled as linear trends over the tracks shown, and sea level time series were derived in 2° longitude by 1° latitude bins within the outlined boundaries.

The combination of the new Geosat XDRs and T2 GDRs has enabled more accurate recovery of the sea level signal in the tropical Pacific [Cheney *et al.*, 1991c]. It therefore seems worthwhile to see if this is also true for the Atlantic Ocean, especially in the Gulf of Guinea where previous studies have shown that the altimetric signal is too weak [Ménard, 1988; Arnault *et al.*, 1992b]. In addition, the longer Geosat time series presented here (4.5 years instead of 1 or 2 for the works previously mentioned) allows study of interannual changes.

In the first part of this paper we will present the data processing, followed by a description of the improvements due to the new corrections for the tropical Atlantic oceanic signal. Then we will discuss results with special attention given to the questions raised during the FOCAL/SEQUAL experiment, such as the possibility of interannual events and/or wave propagation in the tropical Atlantic.

2. Data Processing

Geosat sea level time series were computed at NOAA using a combination of crossover and collinear altimeter differences [Miller and Cheney, 1990]. This method provides continuous sea level records over the period April 1985 to September 1989 with a spatial resolution of 2° longitude by 1° latitude. The following Geosat corrections were applied: TOVS/SSMI water vapor, FNOC dry troposphere and inverted barometer, solid and ocean tides, ionosphere, and sea state bias as 1% of significant wave height. The water vapor and orbit error reduction are of primary importance and are discussed further below.

Emery *et al.* [1990] showed that there are significant differences among various altimetric water vapor corrections; models such as FNOC can be in error by as much as 10 cm in the tropics. However, the large-scale component of

this error is removed in the process of adjusting the altimeter profiles to reduce orbit error. This explains how relatively good altimetric results have been previously obtained in tropical regions even in the presence of substantial water vapor error. For example, Arnault *et al.* [1992a], comparing in situ measurements and altimetric data along a ship line crossing the Intertropical Convergence Zone (ITCZ) in the tropical Atlantic, did not notice any significant bias introduced by the water vapor even when the relatively poor FNOC field was used. Nevertheless, it is clear from monthly mean Pacific tide gauge comparisons [Cheney *et al.*, 1991c] that the TOVS/SSMI water vapor field can substantially reduce the final sea level error.

Because of its long wavelength (the dominant error is at 1 cycle per revolution of the satellite), the orbit error is particularly crucial for the studies of large-scale sea level changes, which represent a major part of tropical investigations using altimetry. Classical methods of orbit error reduction (by polynomial fit over long arcs) are effective but raise a related question: how much of the actual ocean signal is also removed by these adjustments? In the Gulf of Guinea it seems clear that the ocean signal derived from previous altimeter studies [Ménard, 1988; Arnault *et al.*, 1992b] is significantly smaller than indicated by historical data. The particular shape of the tropical Atlantic basin makes it difficult to obtain long, uninterrupted altimeter arcs through-out, leading to a more drastic effect of the orbit filter on the oceanic signal. We have addressed this problem by performing the orbit adjustments over two separate regions as shown in Figure 1. The areas were chosen in an attempt to obtain relatively long arcs, about the same length everywhere, and to minimize the effect of large gaps in the altimeter profiles that would otherwise occur over South America and Africa. Because of the more accurate T2 orbit used, the orbit error could be effectively modeled as a linear trend in an attempt to retain as much sea level signal as possible. (The relatively large radial orbit uncertainty in the original Geosat data set required use of quadratic trends.)

3. Improvement of the Atlantic Oceanic Signal

Unfortunately, in situ data are scarce in the tropical Atlantic Ocean during the Geosat lifetime. Therefore comparison between Geosat old/new corrections and conventional data are not easy to obtain. For a large-scale basin-wide approach the only elements of comparison we can get are through climatological in situ data sets or through the results of numerical models. We use here a primitive equation model which has been run at the Laboratoire d'Océanographie Dynamique et de Climatologie for the Observatoire Permanent de l'Océan Atlantique tropical (OPERA) program between January 1982 and December 1990, forced with monthly winds [Morlière *et al.*, 1989]. The 5/500-dbar dynamic height (hereinafter DH) is first computed from the simulated temperature and salinity fields using the Millero and Poisson [1981] state equation. The DH deviation is then obtained using the DH averaged between April 1985 and September 1989 [Arnault *et al.*, 1992b]. The climatology of in situ DH (0/500 dbar) is that of Merle and Arnault [1985] computed on a monthly basis and a 4° in longitude by 2° in latitude grid.

Figure 2 gives for the altimetric new and old data (Figures 2a and 2b, respectively), the DH climatology (Figure 2c).

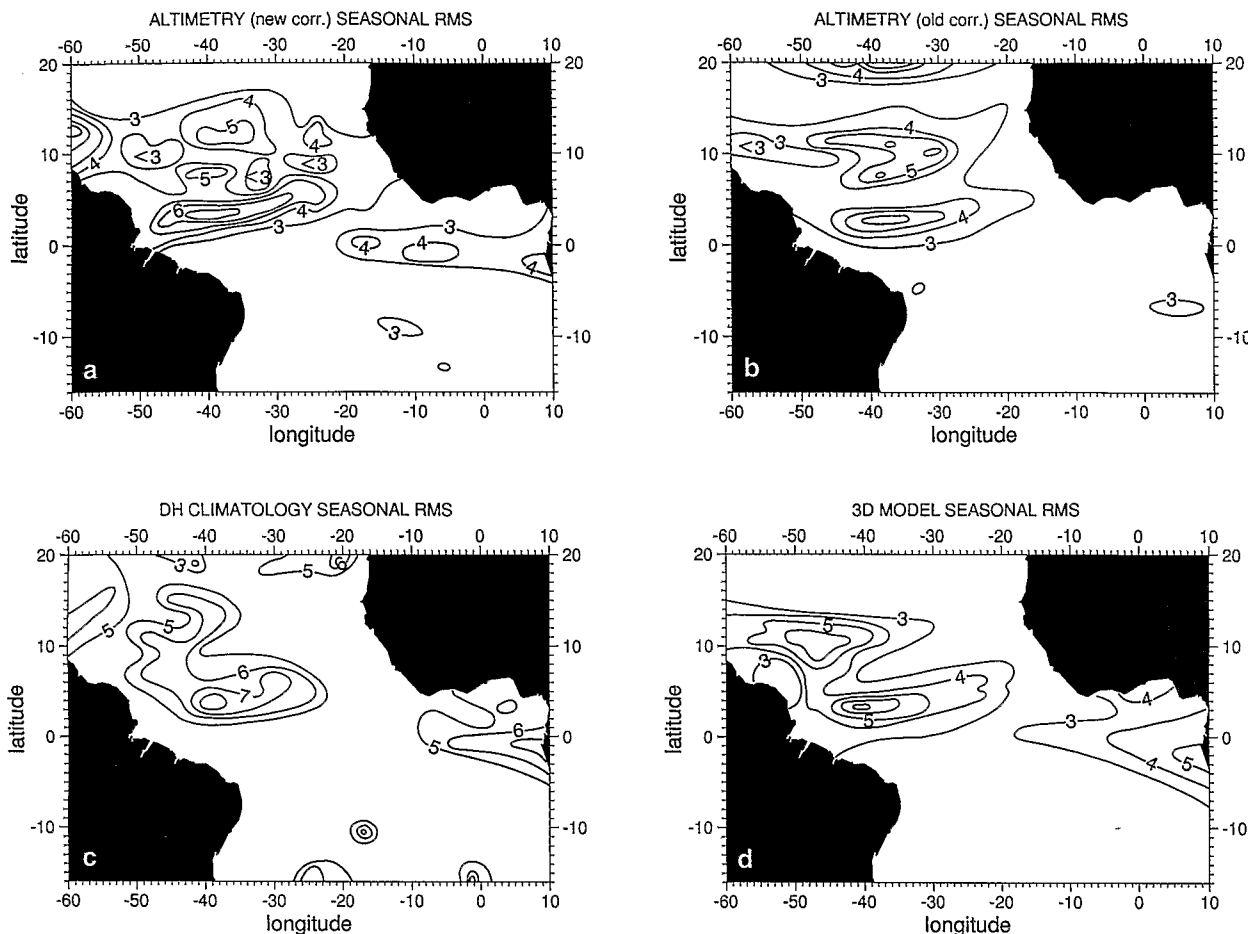


Figure 2. The rms variability (in centimeters) obtained with the Geosat 4.5-year time series (a) using the new Geosat XDRs and T2 GDRs, to be compared with (b) the "old" corrections, (c) the DH climatology of Merle and Arnault [1985], and (d) primitive equation model results forced with 1985–1989 wind stresses.

and the primitive equation model DH (Figure 2d) the rms variability as computed over a mean year. All the figures present the same large variability (over 6–7 cm) in the western area, between 2° and 7°N, 20° and 40°W. Northward, around 10°–12°N, another maximum appears. These large variabilities are related to the seasonal migration of the ITCZ. In the Gulf of Guinea the DH variability reaches 6–7 cm along the African coast. The model gives only 4–5 cm, and the new altimetric data set gives only 4 cm. But these values constitute a slight improvement compared to the complete missing signal in the old Geosat data.

As mentioned before, in situ data in this region for this period are few. The large network of tide gauges deployed during the FOCAL/SEQUAL experiment in 1982–1984 is now out of use (G. Mitchum, personal communication, 1994). The only tide gauge records long enough to be significantly used for such a comparison are located in the Gulf of Guinea, one at Principe Island (1°39'N to 7°26'E) and another one at Pointe Noire (4°48'S to 11°51'E) (courtesy of J. M. Verstraete, 1992). Figure 3 (top) gives the comparison of the altimetric signal (old and new corrections) with the tide gauge sea level deviation, on a monthly basis, between January 1985 and September 1989 at Pointe Noire. The tide gauge and the new Geosat signal vary in phase ($r = 0.66$), with a slight improvement compared with the old altimetric

data ($r = 0.51$), but the amplitude of this signal remains less for altimetry (rms difference = 5.4 cm) even if the use of the new corrections improves it (rms difference = 7.1 cm for the old data). However, we must keep in mind that the location of the Pointe Noire tide gauge (in the far end of the harbor) is not optimal for such a comparison. In such an area the signal can be affected by phenomena other than those captured by a coastal instrument. It is noteworthy that the agreement between the primitive equation model results and the Pointe Noire tide gauge is not better: the rms difference between the model and the tide gauge is 5.4 cm and the correlation is 0.48, when the comparison between altimetry and model at the same location gives 3.7 cm for the rms difference and 0.6 for the correlation. Thus the dynamics sampled by the altimeter or reproduced by the model look more similar compared to each other than with the tide gauge signal. This reveals how difficult a comparison can be between an in situ measurement sampled at a single location and a signal averaged over a surrounded area. In that sense the tide gauge of Principe Island, located offshore on a small island in the Gulf of Guinea, can be more promising (Figure 3, bottom). Effectively, the two amplitudes of the signal at Principe (new Geosat and tide gauge) are in much better agreement than when using the old corrections. The rms difference is now 3.2 cm instead of 4.5 cm with the old

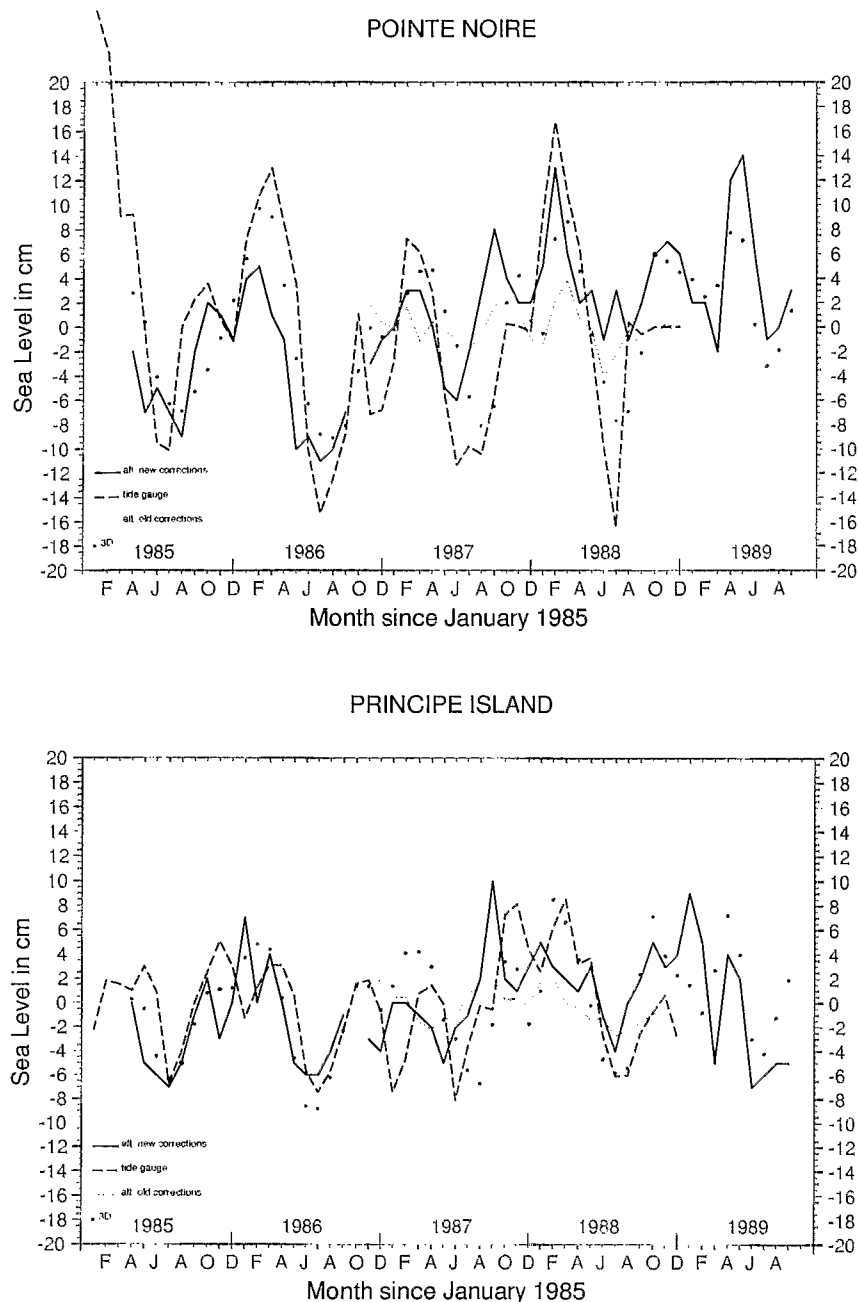


Figure 3. Sea level record in the Gulf of Guinea at Pointe Noire and Principe Island from tide gauge data (courtesy of J. M. Verstraete, 1992; long-dashed line), Geosat using the new analysis (solid line), and Geosat altimetric data using FNOC water vapor and a less accurate orbit and shorter arcs (short-dashed line). Units are in centimeters. Improvement in the phasing and amplitude of the new altimetric signal is evident. For comparison, primitive equation model results are also given (circles).

corrections at the same point, and the correlation remains good ($r = 0.56$) and significantly increased compared to old data ($r = 0.32$). The results obtained with the model are quite similar: the rms difference model/tide gauge is 3.6 cm and the correlation is 0.6.

The final step of our comparison is given in Figure 4, which presents the correlation and rms differences between altimetry and the primitive equation model. The correlations are particularly high (reaching more than 0.7) along the equator (between 8°N and $2^{\circ}\text{--}8^{\circ}\text{S}$), then between 10° and

15°N . The rms differences reveal major discrepancies (>6 cm) along the northwestern American coast ($50^{\circ}\text{--}60^{\circ}\text{W}$, $5^{\circ}\text{--}10^{\circ}\text{N}$), but the differences are low over a large part of the basin, generally less than 3 cm. We have selected two points for our comparison: one located in a "good" area (rms < 3 cm, correlation > 0.7) at 0°N to 2°W and a second one in a "bad" area (rms > 6 cm, correlation < 0.5) at 8°N to 49°W . In both cases the altimetric signal is improved using the new corrections. For the "worst" comparison, in the west, the rms difference between altimetry and model is now 5.8 cm

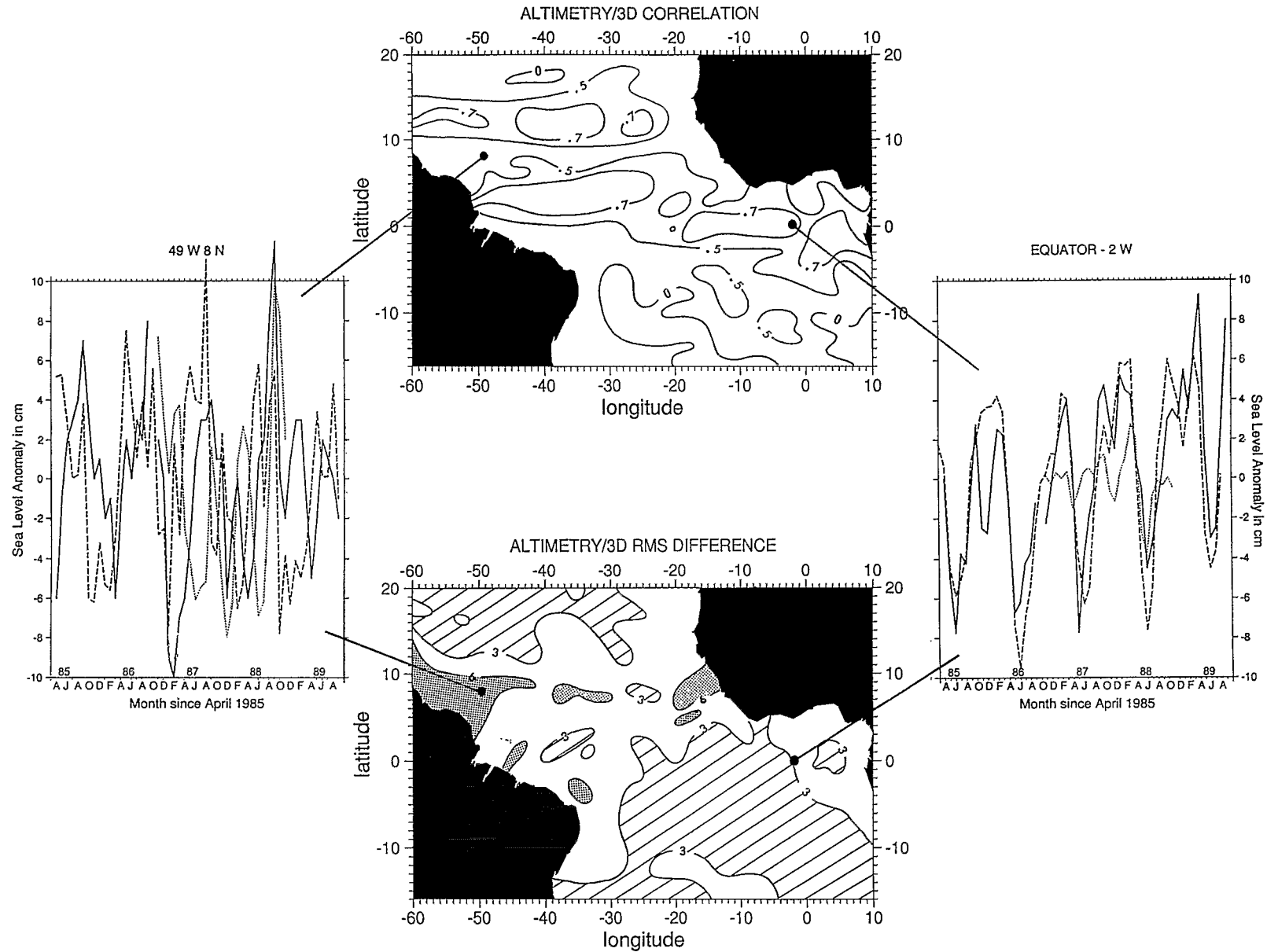


Figure 4. (Top) Correlation and (bottom) rms differences between the Geosat sea level using the new analysis and the results of a primitive equation model. A comparison (right) in the Gulf of Guinea (0°N, 2°W) where the agreement is “good” and (left) in the western area (8°N, 49°W) where it is “bad” between Geosat using the new analysis (solid line), Geosat using old corrections (dashed line), and the model (dotted line) is also given.

Table 1. Explained Variance of the Seasonal and Interannual Atlantic Sea Level Signals for the First EOFs

| | Seasonal | | Interannual | |
|-------|-----------------------|----------------|-----------------------|----------------|
| | Variance per Function | Total Variance | Variance per Function | Total Variance |
| EOF 1 | 46% | 46% | 27% | 27% |
| EOF 2 | 25% | 71% | 8% | 35% |
| EOF 3 | 10% | 81% | 6% | 41% |

instead of 8.3 cm using old data, and the correlation has gone up from 0.0 to 0.2. From Figure 4 it is evident that the disagreement here is not a problem of amplitude but of high-frequency oscillations in the two signals which sometimes occur out of phase. In the Gulf of Guinea the new altimetric data led to a 3.1-cm difference and 0.68 correlation instead of 3.9 cm and 0.32 for the old version.

Of course, comparison with an ocean model simulation does not necessarily confirm the existence of a real oceanographic feature, but these basinwide results, together with the isolated tide gauge comparison, are good enough to strengthen our feeling that the new Geosat corrections improve the quality of the sea level signal in the tropical Atlantic, as was the case for the tropical Pacific. It follows that processes with small amplitudes, such as wave propagation and interannual events, can now be more thoroughly investigated.

4. Results of the Sea Level Analysis

4.1. Seasonal Variability

An empirical orthogonal function (EOF) analysis was performed first on the seasonal cycle which can be obtained by averaging the altimetric deviation between April 1985 and September 1989. As shown in Table 1, only three EOFs are needed to describe about 80% of the seasonal variance. The EOFs have large spatial scales, and their temporal behavior is coherent (see Figures 5–7). The first EOF spatial structure presents two maxima which are located around 2°–3°N and 10°–12°N (Figure 5a). These maxima are opposite, so that when the time series reaches positive maximum in October (Figure 5b), the sea level rises at 2°–3°N (maximal positive sea level deviation, hereinafter referred to as SLD) and falls at 10°–12°N (maximal negative SLD). This is the meridional "tilting" of the tropical Atlantic Ocean along the mean location of the ITCZ [Merle, 1980], which partly induces the North Equatorial Countercurrent (NECC) variability [Garzoli and Katz, 1983]. The spatial structures of the second EOF (Figure 6a) are mostly confined in the equatorial band (5°N to 5°S). The strongest extremum occurs along the equator, in the Gulf of Guinea. Combined with the time series, it indicates negative values in June–July as opposed to the rest of the basin (Figure 6b). This is the signal of the equatorial upwelling which occurs every year in the Gulf of Guinea during the boreal summer, with a more rapid buildup (4 months) than decay (6 months) phase. The third EOF clearly reveals a semiannual signal (Figure 7b). The spatial structures present extrema in the northwestern part of the basin and in the Gulf of Guinea (Figure 7a). Figure 8 gives the energy spectra for these two regions. Two energetic

peaks are clearly shown at 6 months and 12 months, reaching the same energy level (around 100 m² cycle⁻¹ month⁻¹). These semiannual signals in these two parts of the basin are well known features of the tropical Atlantic Ocean, especially the one occurring in the Gulf of Guinea which corresponds to a second upwelling signal during boreal winter.

This EOF analysis of the altimetric seasonal signal presents familiar characteristics which have been observed using conventional data. For example, with the same kind of analysis performed on DH climatology, Duchêne and Frankignoul [1991] found that 79% of the seasonal signal was recovered with three EOFs. The spatial and temporal structures associated with their analysis are in very good agreement with ours (see Duchêne and Frankignoul, 1991, Figure 2), the first EOF being the signal of the meridional tilting along the ITCZ, the second one being those of the equatorial upwelling, and the third one being the semiannual signal.

4.2. Interannual Variability

The same EOF decomposition has been applied to the whole 1985–1989 series minus the seasonal cycle to characterize interannual phenomena. To avoid confusion, we will use the following terminology: sea level deviation (SLD) will refer to the "total" altimetric signal and sea level anomaly (SLA) will refer to the "interannual" part of it. Figure 9 gives for two different locations in the tropical Atlantic Ocean the comparison between the total signal and the seasonal and interannual components. These locations are characteristic of regions whose dynamics are crucial for the tropical Atlantic Ocean. The Gulf of Guinea is the center of the equatorial upwelling, occurring twice a year, in summer and then in winter. The region is also known to have important year-to-year fluctuations: as in 1984, during the FOCAL/SEQUAL experiment, abnormally warm waters have overrun most of the area during the first part of the year. The other location, in the NECC core, is interesting because of the role of this eastward current in the redistribution of heat through oceanic circulation. Either in the Gulf of Guinea or in the NECC region the amplitude of the interannual part, compared with the seasonal or the total signal, is far from negligible and well above the mean accuracy (3–4 cm) attributed to altimetric data. This is confirmed by Figure 10, which presents the ratio between the seasonal and the interannual rms variability. The ratio is above 1 (seasonal variability > interannual variability) only in the northwestern basin (0°–15°N × 25°–60°W) and in the southeastern one (0°–10°S × 20°W to 10°E). Elsewhere, the interannual variability between April 1985 and September 1989 is of the same order as or greater than the seasonal one.

Table 1 gives the percentage of variance explained by the first three EOFs computed on the SLA. The first function explains 27% of the interannual variance. The time series associated with this EOF (Figure 11b) presents a clear trend, first between April 1985 and February 1987 and then between March 1987 and December 1988 with an even more pronounced slope. A minimum is reached between January and April 1989. The spatial structures associated with this time series clearly identify a mass redistribution between the equatorial region 10°N to 10°S and the northern and southern ones 10°N to 30°N, 10°S to 30°S. This redistribution between the equatorial region and the northern and southern ones is also evidenced by space-time plots along the equator, 15°N, and 15°S. The interannual anomalies along the equator are

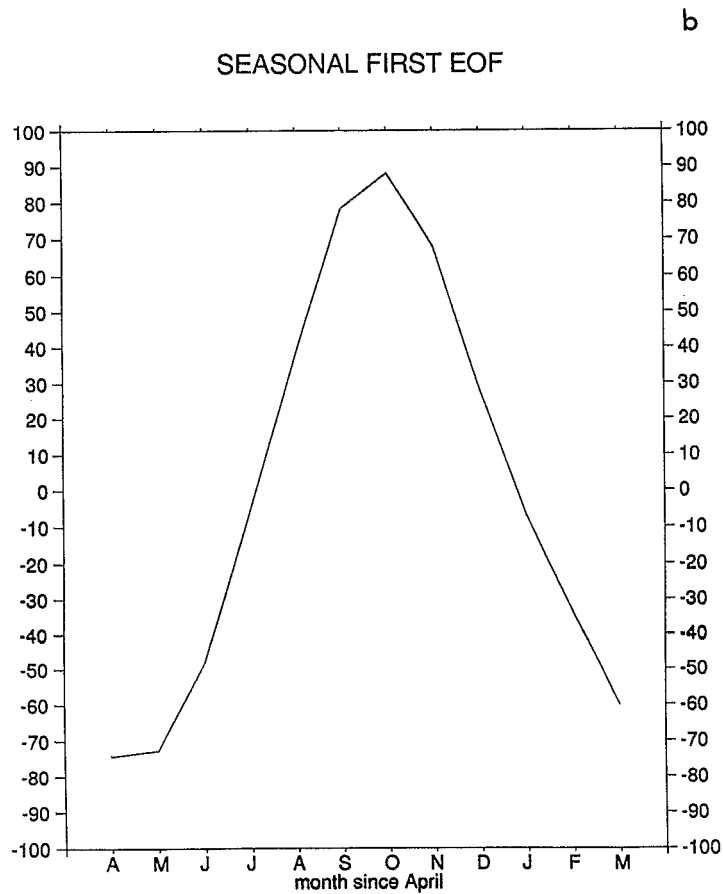
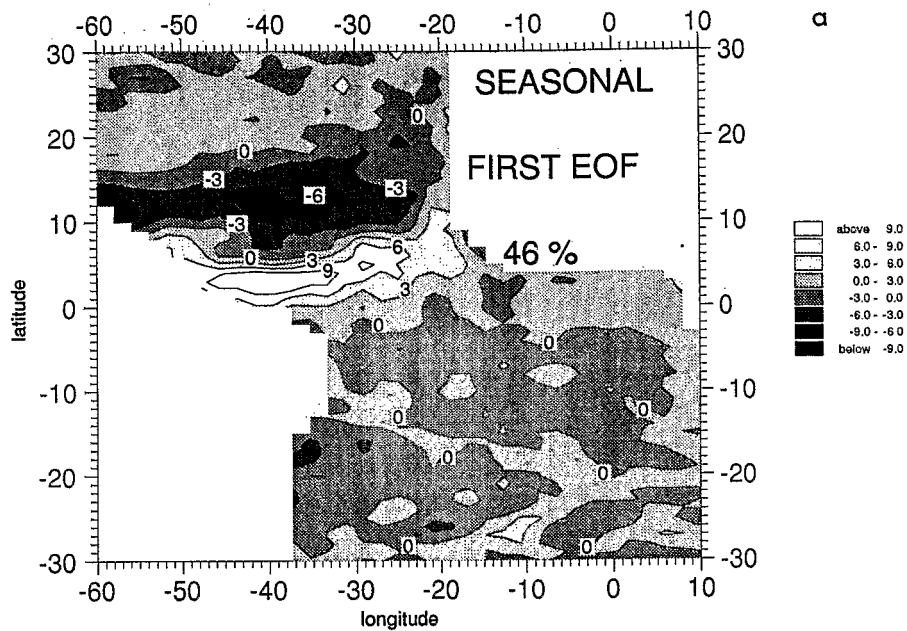
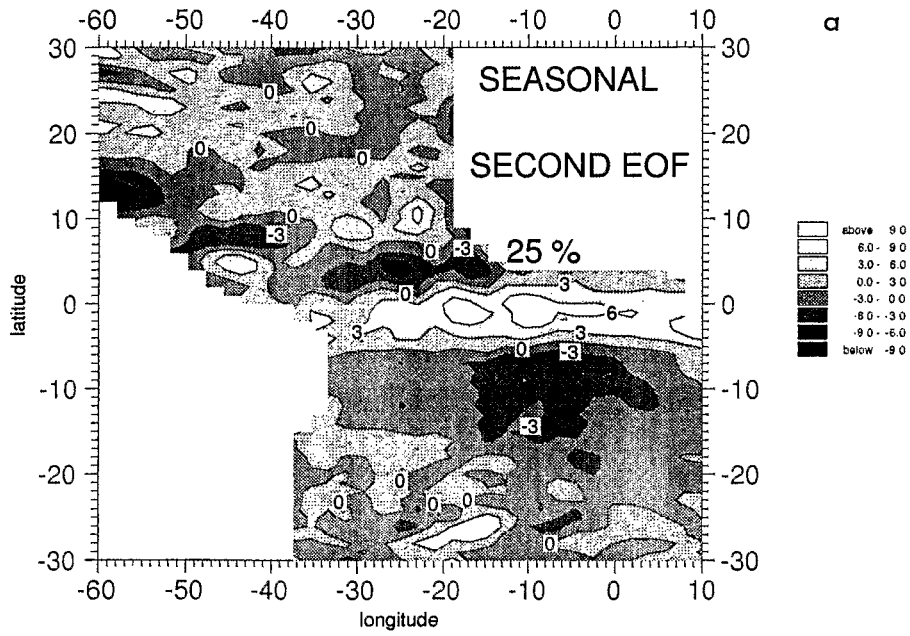


Figure 5. First empirical orthogonal function characteristics: (a) spatial and (b) temporal structures of an analysis performed on the seasonal altimetric signal. This EOF reveals the meridional tilting of the ocean along 5°N.



SEASONAL SECOND EOF

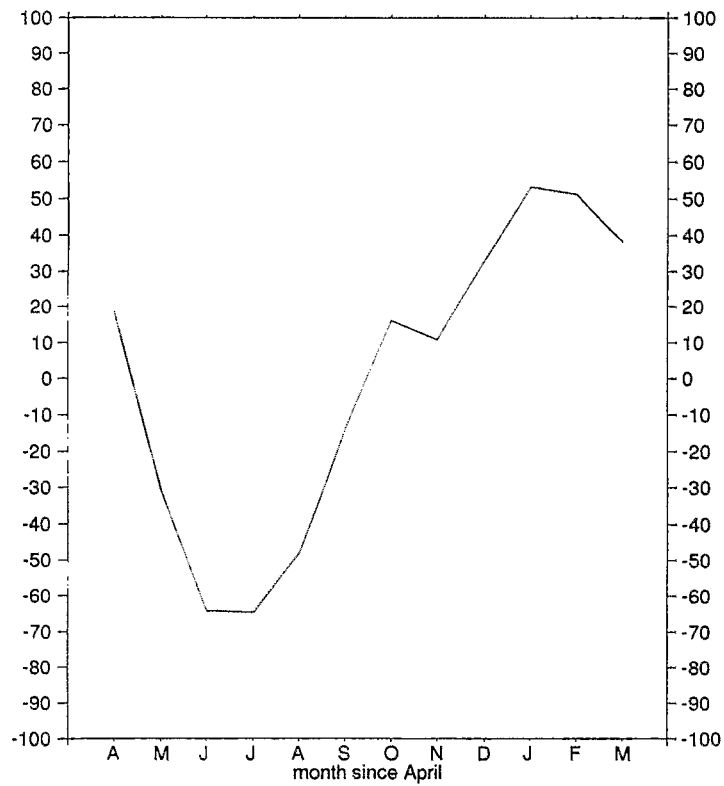
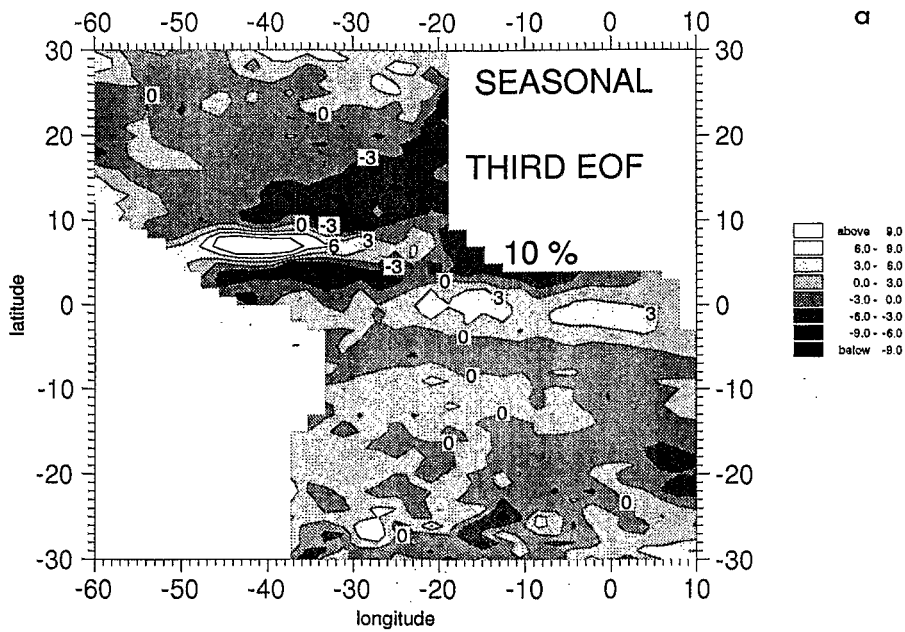


Figure 6. Same as Figure 5 but for the second EOF. It reveals the zonal tilting of the ocean associated with the upwelling signal.



b

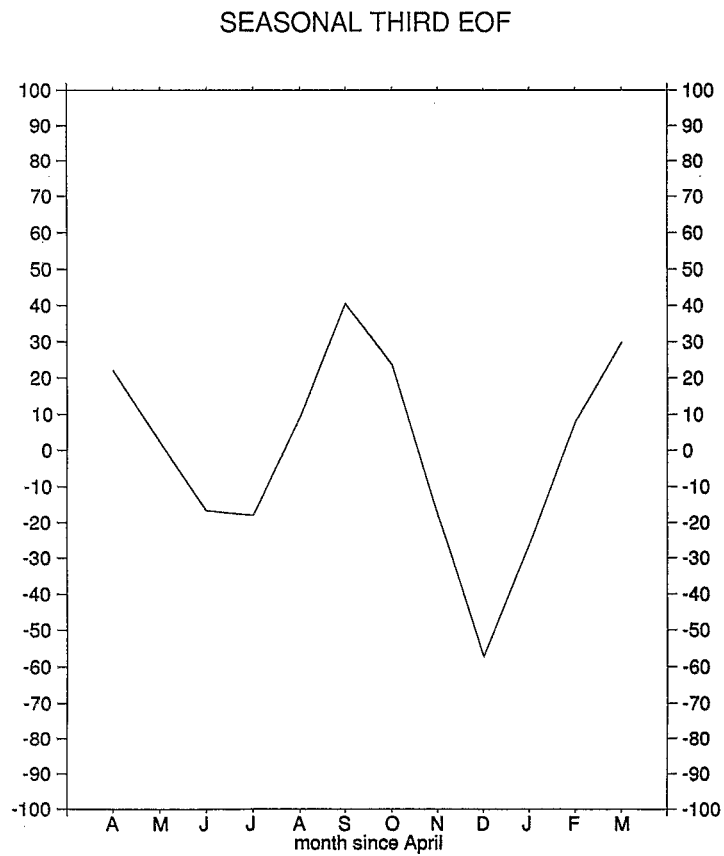


Figure 7. Same as Figure 5 but for the third EOF. It reveals the semiannual characteristic of the tropical Atlantic signal.

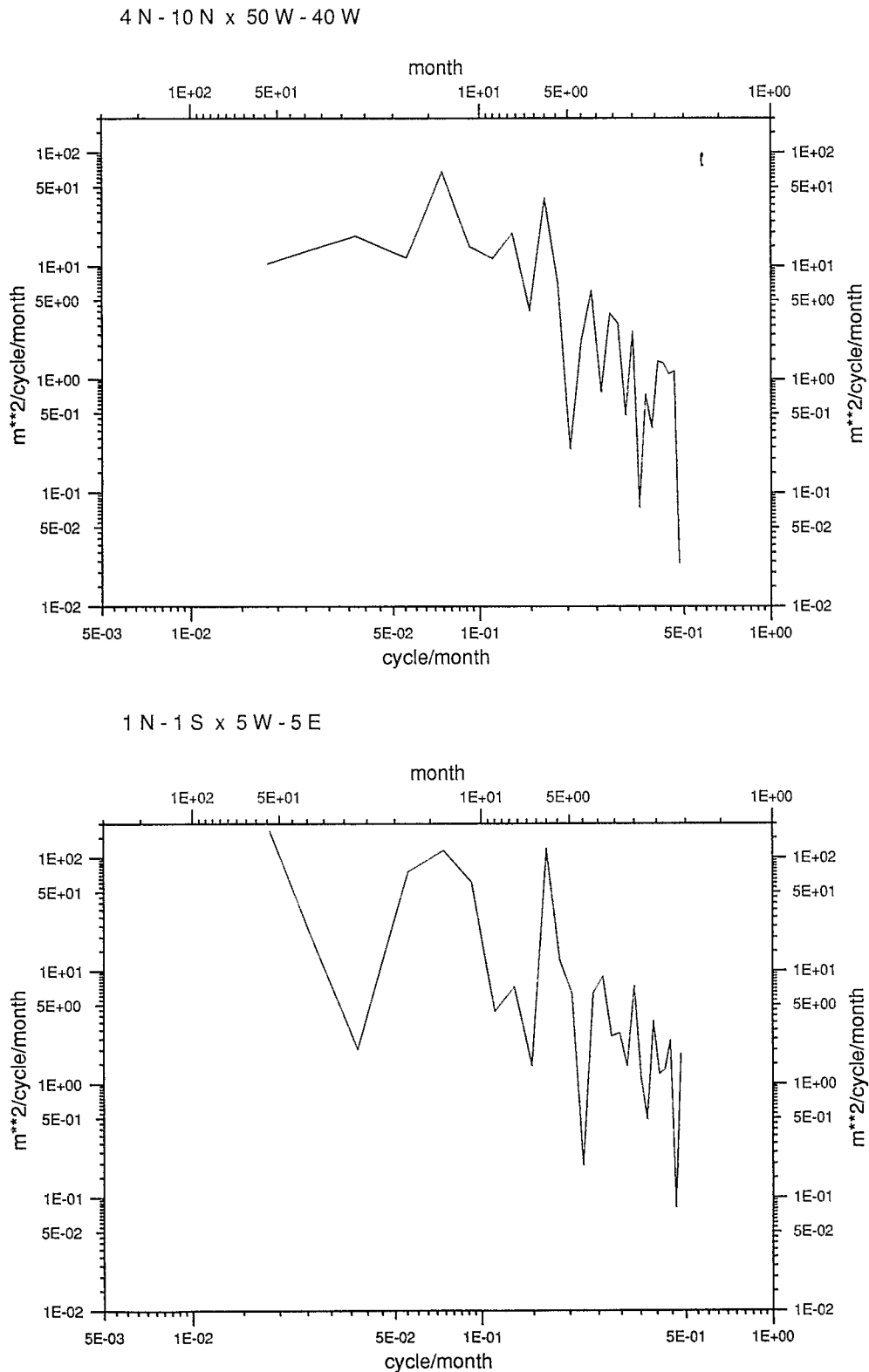


Figure 8. Power spectra of the Geosat time series for (top) the northern region (4°N to 10°N , 50°W to 40°W) and (bottom) the equatorial region (1°N to 1°S , 5°W to 5°E) revealing the importance of the semiannual signal in these two parts of the Atlantic basin.

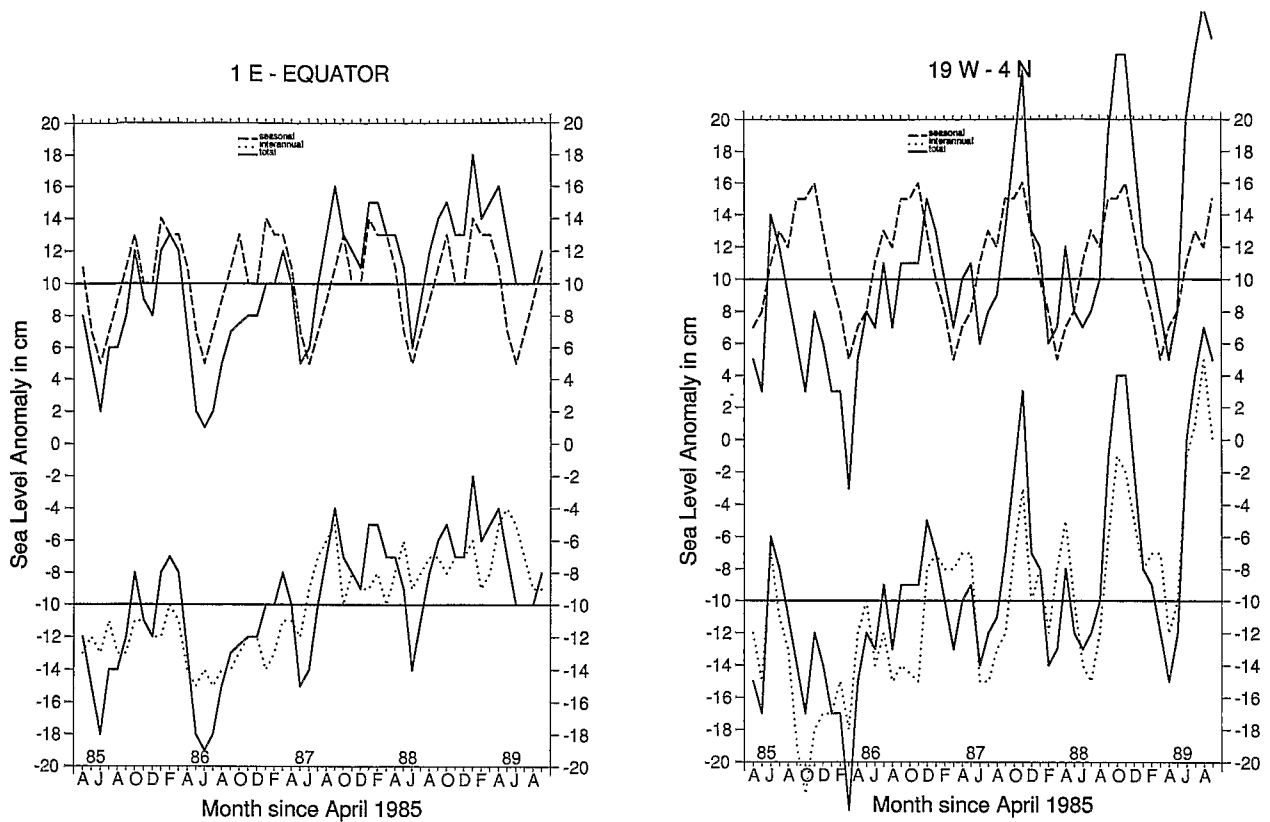


Figure 9. Seasonal (dashed line) and interannual (dotted line) part of the total signals (solid line) as obtained from Geosat data for different locations: 19°W–4°N and 1°E–0°N. Units are in centimeters.

mostly negative between April 1985 and May–June 1987 and mostly positive from May–June 1987 to September 1989 (Figure 12), when the signals along 15°N and 15°S particularly (not presented here) are clearly opposite. Also interesting to note is the presence along the equator of eastward propagation in March–May 1986, March–June 1987, and March–April 1989 more particularly.

5. Discussion

Until recently, it has been widely assumed that the tropical Atlantic signal was mostly seasonal, contrary to the Pacific Ocean with its strong interannual signals (El Niño events). This assertion was primarily based on theoretical studies of the adjustment time scale of the basin [Philander, 1979; Cane and Sarachik, 1981] and on the analysis of sea surface temperature (SST) data in the Gulf of Guinea by Merle et al. [1979]. These authors found that the annual signal had a larger amplitude than the interannual anomalies and a standard deviation about 5 times higher than the standard deviation of interannual anomalies. However, they noticed that when interannual variabilities occurred, they had a large spatial extent and could affect the whole basin for several months or a year. This led Hisard [1979] and Merle [1982] to make the hypothesis of an Atlantic “El Niño” which could refer to the presence of warm water in the Gulf of Guinea in boreal spring, when the equatorial upwelling usually develops. In preparation for the FOCAL experiment, Picaut et al. [1984] analyzed SST data covering the 1964–1979 period. They pointed out that the interannual

variability was maximum in regions where the amplitude of the seasonal signal was large, for example, the seasonal upwelling zones. Most of this interannual variability was associated with changes in the amplitude, timing, and duration of the cold season. But unlike Merle et al. [1979], Picaut et al. [1984] found that the ratio between seasonal and interannual variability was always between 2.5 and 4 (instead of 4–5) inside the Gulf of Guinea. They explained this disagreement by the fact that Merle et al.’s study was based

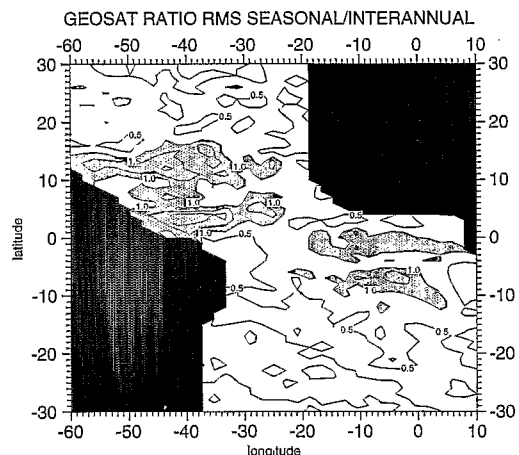


Figure 10. Ratio between seasonal and interannual rms variability as obtained from Geosat.

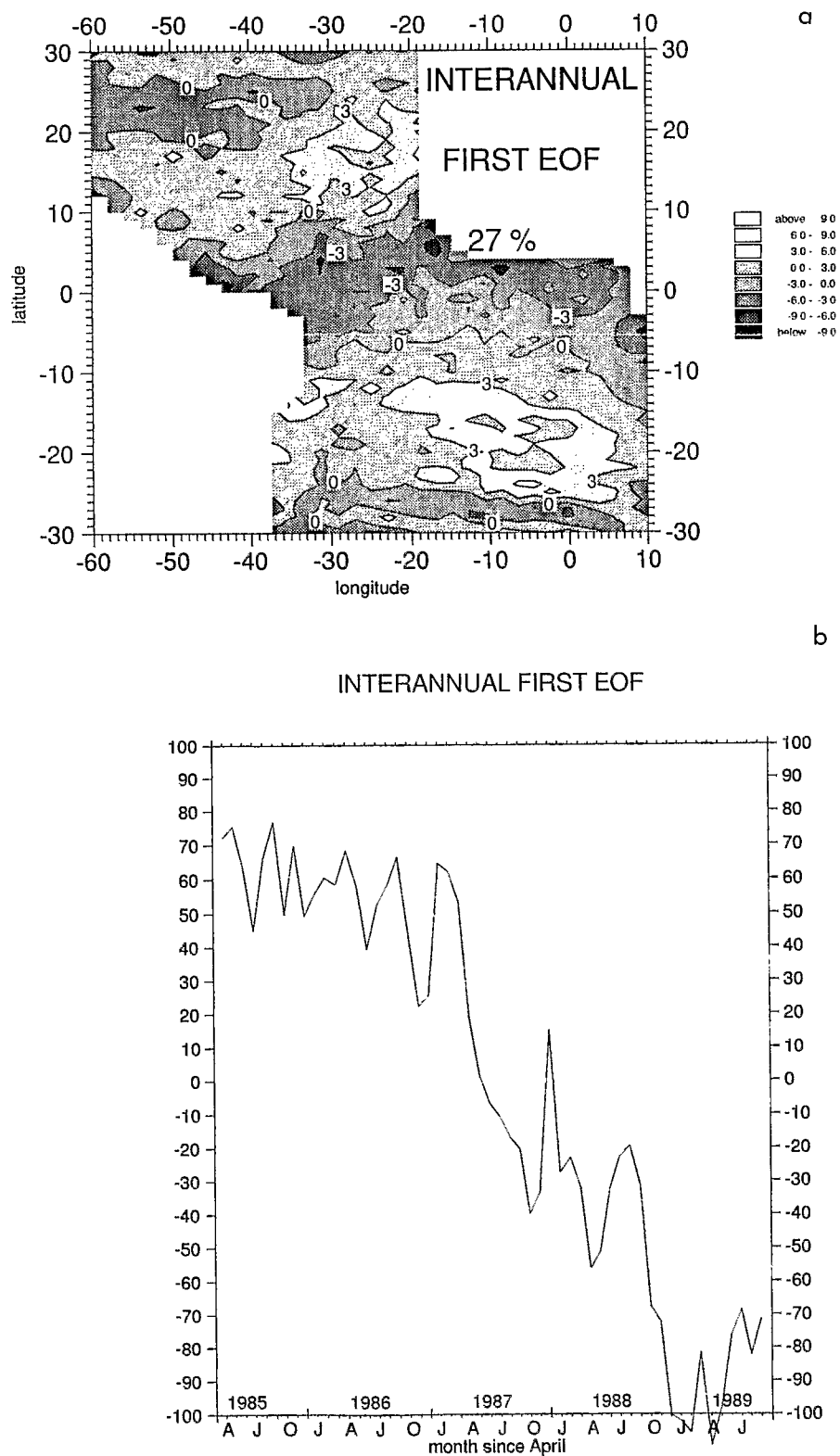


Figure 11. Same as Figure 5 except for the interannual signal. A trend starting in early 1987 for the equatorial region as well as a mass redistribution of the water between the northern and southern regions and the equatorial one is clearly shown.

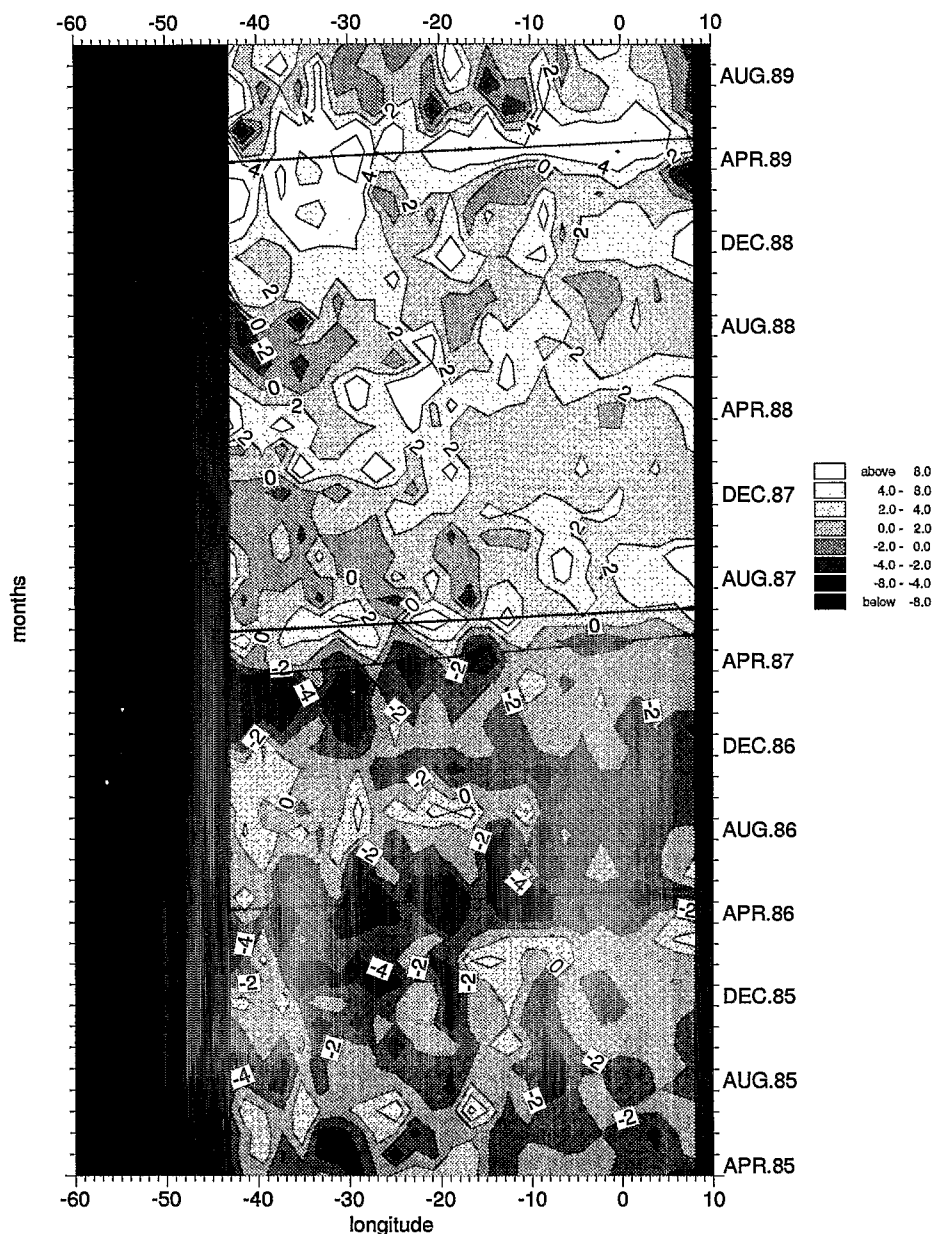


Figure 12. Time-longitude diagram of the interannual Geosat sea level anomaly along the equator (in centimeters). Negative anomalies (solid and densely stippled) and positive anomalies (open and lightly stippled) are shown. The trend of this region is noticeable. Characteristic propagation speeds of 2 m s^{-1} and 1.30 m s^{-1} are also drawn on the figure.

upon February and August data only, two months in which interannual SST changes are small. Unusual meteorological and oceanographic conditions over the tropical Atlantic detected during the intensive FOCAL/SEQUAL experiment in 1984 definitely evidenced the presence of interannual events in this ocean (see, for example, the special issue of *Nature*, 322(6076), 1986), even if these events have a smaller extent than the Pacific El Niño. Besides, most of the Atlantic interannual events which have been clearly identified up to now, for example, 1963–1964, 1967–1968, and 1983–1984 [Weare, 1977; Lamb, 1978; Servain and Legler, 1986], follow Pacific events. Moreover, a global experiment gathering several modeling teams all over the world has been initiated to try to identify whether the Atlantic and Pacific phenomena

could be related (J. Servain, personal communication, 1993). This relationship, if it exists, is not the focus of this paper, but it is worth noting. Therefore unusual conditions as revealed by our altimetric measurements in the tropical Atlantic in 1987–1988 do not look strange, occurring as they do after the Pacific 1986–1987 El Niño. Furthermore, in a recent paper, Katz [1993], using inverted echo sounders at 3°N to 38°W and 9°N to 38°W during 6 years and 10 months, shows that if the annual signal dominates as expected in the NECC variability, the interannual variability is of comparable magnitude. Two years, 1983 and 1987, are noted as years of sharp increase in the interannual signal (periods immediately following El Niño events in the Pacific). In this 6-year record of NECC index, there are two maxima both occurring

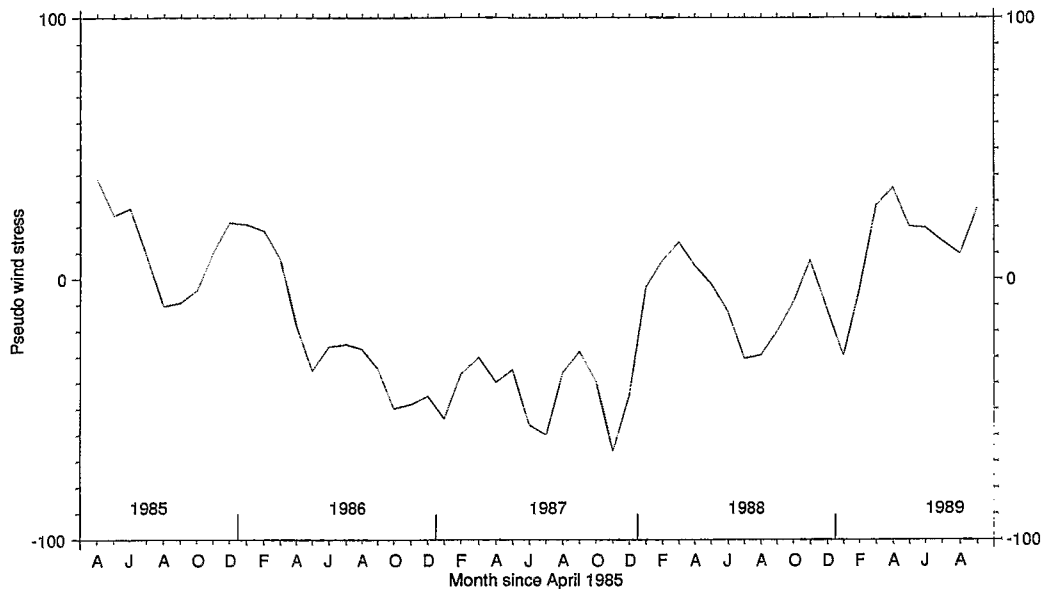


Figure 13. Evolution between April 1985 and September 1989 of the interannual anomalies of the pseudo wind stress zonal component (in square meters per square second) along the equator. A low-pass filter to this series has been applied. This component significantly decreased (positive anomaly) after 1987, in agreement with the Geosat sea level anomaly positive increase.

about one-half year or less after the two minima in the Southern Oscillation Index, the latter presumably affecting the global atmospheric circulation.

However, because of the many uncertainties associated with altimetric sea level, we must determine whether this trend observed from Geosat in the tropical Atlantic between spring 1987 and winter 1988 was due to one of the various corrections (water vapor, for example, which is based on the TOVS data set prior to July 1987 and SSMI data after) or to a satellite sampling artifact. The first idea is to look at a potential signal in the wind stress forcing. J. Servain kindly provided us his wind analysis for the 1985–1989 period. These are ship winds objectively mapped on a $2^\circ \times 2^\circ \times$ month basis [Servain *et al.*, 1987]. The time series starts in January 1964 and ends in December 1992, quite a long duration to compute a reliable mean seasonal cycle and therefore to obtain the interannual variability of these winds. Figure 13 shows the interannual anomaly of the wind pseudostress zonal component averaged along the equator between 2°N and 2°S . The zonal wind strengthens from April 1985 to spring 1987 and then weakens until early 1989. This weakening trend occurs just when the altimetric sea level indicates a general increase for the equatorial area. Thus from a dynamical point of view the two kinds of data are in good agreement: when the winds relax along the equator, the zonal pressure gradient, no longer equilibrated by the wind, weakens too. Warm waters piled up along the South American coast tend to flow back to the east, resulting in a sea level increase. It could also be worthwhile to look at the results of the three-dimensional model forced with these winds and run at Laboratoire d'Océanographie Dynamique et de Climatologie (LODYC) by A. Morlière [Morlière *et al.*, 1989]. As mentioned earlier, from the temperature and salinity fields we obtained dynamic height (referenced to 500 dbar) series over the tropical Atlantic and performed the

same EOF analysis as our altimetric data. The first EOF accounts for 25% of the interannual variance, and the temporal signal and spatial structures (Figure 14) reveal the same trend of the equatorial area starting in spring 1987. It is therefore obvious that this general trend which affects the tropical Atlantic Ocean from early 1987 until winter 1988 is not an artifact of satellite data but a real oceanographic feature such as the one detected in 1984.

Wyrki [1985], using the Pacific tide gauge network, showed that at the end of El Niño the equatorial Pacific was depleted of warm water which was lost toward higher latitudes. Miller and Cheney [1990] estimated the same transport from Geosat data in the Pacific during the 1986–1987 El Niño. They found a clear exchange of water involving principally the equatorial and the north equatorial regions. Because our EOF analysis also suggests such an exchange, we computed the Atlantic upper layer transports. Because of the simple relation between thermocline depth and sea level height, the upper layer volume can be approximated by [Wyrki, 1985]

$$H = (\rho/\Delta\rho) \iint h \, dx \, dy$$

where ρ is the sea water density, $\Delta\rho$ is the density difference between upper and deeper waters, and h is the SLA. We fixed the latitudinal limits of our bands following the spatial structure revealed by the EOF analysis, i.e., 10°N to 10°S for the equatorial zone and 10°N to 30°N and 10°S to 30°S for the northern and southern ones. In the equatorial region, there is an accumulation of water between 1987 and 1989 (Figure 15) increasing from about -1.5 to $1.5 \times 10^{14} \text{ m}^3$. This corresponds to a change in sea level of 6 cm. This is opposite in phase to the northern and southern region (correlation approximately -0.85).

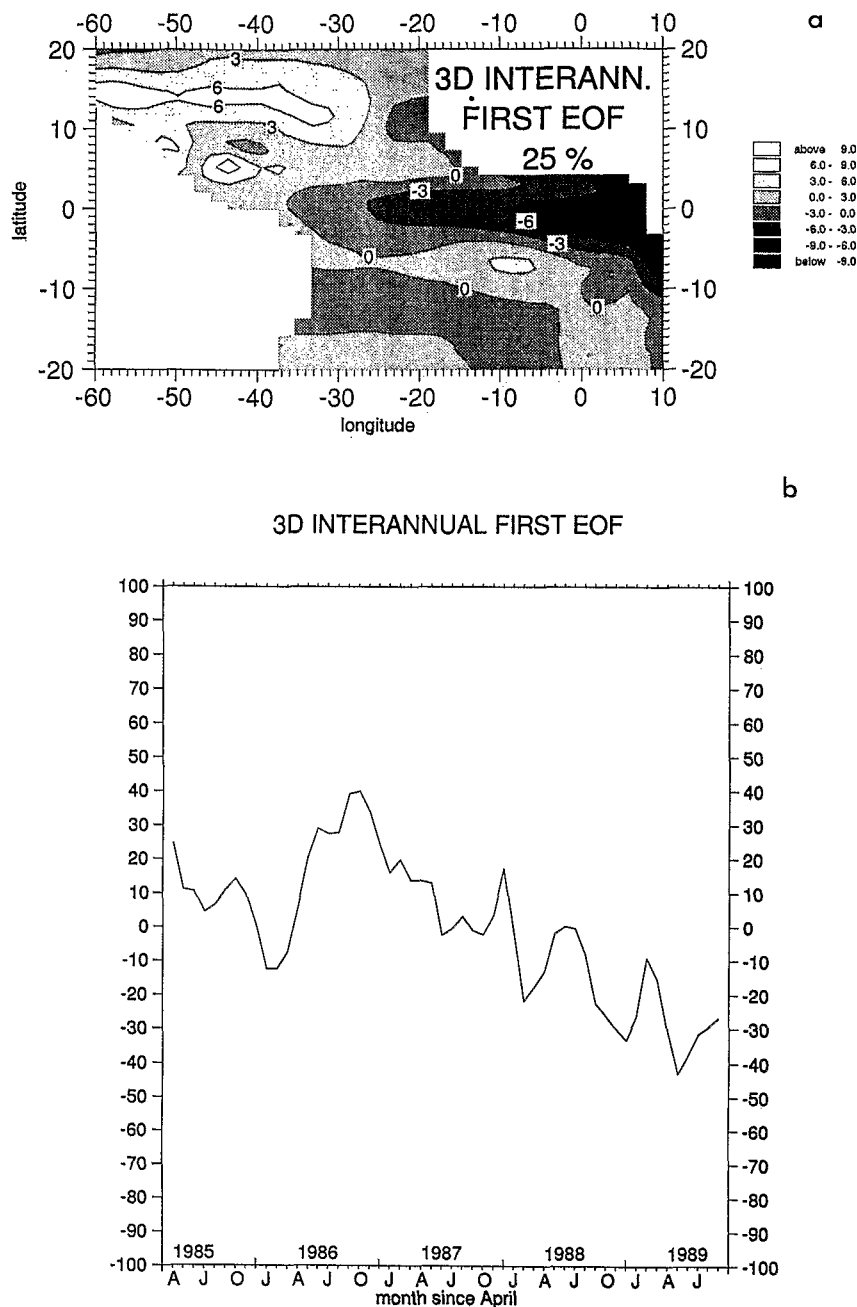


Figure 14. Same as Figure 11 except for the primitive equation model results.

As stated previously, in situ data are too scarce in 1985–1989 to allow such a global basinwide computation. The largest file we can use is obtained from the selected expendable bathythermograph (XBT) surveys (courtesy of J. P. Rebert, ORSTOM, 1993). In order to keep the maximum information from the data while avoiding possible artifact due to the irregular data distribution (mainly gathered along ship lines), we computed a mean 0- to 800-dbar heat content over three regions: 10°–20°N, 5°N to 5°S, and 15°–20°S. Figure 16 gives the interannual anomalies between April 1985 and September 1989 of these XBT heat contents. The northern and southern regions clearly indicate a general decreasing trend while the equatorial area increases, especially between late 1986 and 1989. A linear fit gives for

these trends the following values: -16 for the northern band, -7 for the southern one, and 6 for the equatorial area. The correlation between the extra-equatorial and the equatorial areas is negative and around -0.5 . It therefore appears that following the Pacific El Niño event in 1986–1987, the tropical Atlantic Ocean also experienced abnormal conditions, with a clear warming trend in the equatorial region from mid-1987 until late 1988.

6. Summary and Conclusion

We have used Geosat sea level data from April 1985 to September 1989 to derive seasonal and interannual anoma-

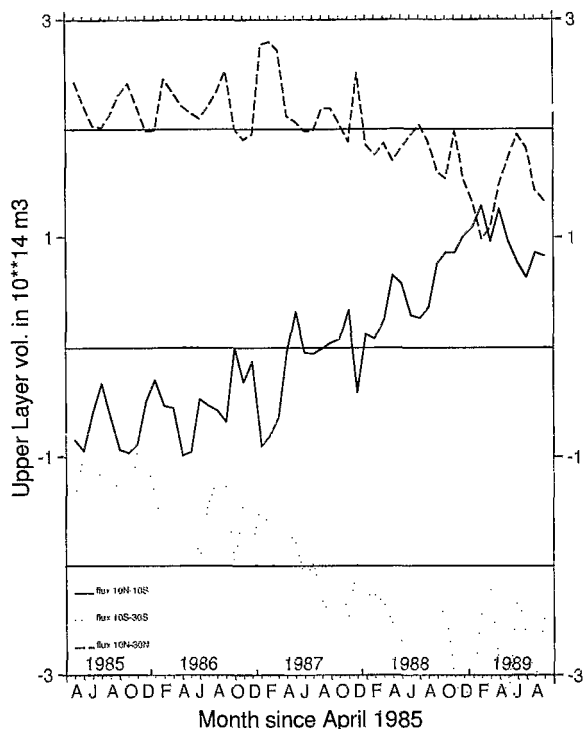


Figure 15. Upper layer volume interannual anomaly computed from the Geosat series for the equatorial 10°N to 10°S region (solid line), the northern 10°N to 30°N region (dashed line), and the southern 10°S to 30°S region (dotted line). Units are in 10^{14} m^3 . To clear the picture, the northern and southern signals have been shifted by 2 cm. The mass exchange is clearly evident.

lies in the tropical Atlantic ocean. The new T2 GDRs for Geosat, with more accurate water vapor and orbit, significantly improve the recovery of the oceanic signal from altimetry, especially in the eastern part of the basin. The comparison between the new altimetric signal and two tide gauge data sets in the Gulf of Guinea gives a correlation of 0.66 and 0.56 (instead of 0.51 and 0.32 with previous altimetric data) and a mean rms difference of 5.4 cm and 3.2 cm (instead of 7.1 and 4.5 cm). This improvement is also confirmed by the results of a primitive equation model, with a mean rms difference about 3–4 cm and a correlation of about 0.7, instead of 4–5 cm and 0.3.

EOF analysis performed over the seasonal cycle of the altimetric data shows the meridional “tilting” of the tropical Atlantic Ocean along the mean location of the ITCZ (first EOF), the mass redistribution due to the equatorial upwelling signal peaking in June–July (second EOF), and a semiannual signal in the northwestern part of the basin and in the Gulf of Guinea (third EOF).

The same EOF decomposition applied to characterize interannual phenomena reveals (first EOF) a clear trend between March 1987 and December 1988 and a mass redistribution between the equatorial region (10°N to 10°S) and the northern and southern ones (10°N to 30°N and 10°S to 30°S). This trend, in good agreement with wind data and numerical model results, is therefore not the result of artifacts or errors in altimetric data processing. The interannual anomaly of the equatorial upper layer volume increases from April 1985 to December 1988 while the northern and south-

ern regions exhibit corresponding decreasing volumes. Using the few XBT lines covering the spatial and temporal areas, we also find these trends and basinwide exchange from 0- to 800-dbar heat content. Propagations along the equator are also seen in spring 1986, 1987, and 1989.

The most interesting result from these Geosat data supports the ideas formulated during the FOCAL/SEQUAL experiment that interannual events do occur in the tropical Atlantic. The advantage of altimetry lies in its unmatched coverage, enabling comprehensive, large-scale studies. As was the case in 1984 with the intensive survey of FOCAL/SEQUAL, Geosat has captured in 1988 a rather large anomaly in the Gulf of Guinea. The next step for this work could be studying the relationship between the Pacific and the Atlantic. Most Pacific El Niño events in recent times (1963–1964, 1967–1968, 1976–1977, 1982–1984, 1986–1988) have been followed by several months by interannual anomalies in the Atlantic [Weare, 1977; Lamb, 1978; Servain and Legler, 1986; Katz, 1993]. The data coverage of satellite techniques, together with in situ measurements and numerical model results, will offer a unique way of testing the interconnection hypothesis. Hopefully, the new information obtained with Geosat will soon be extended using the altimeter data from ERS 1, launched in 1991, and refined with the more accurate altimeter data anticipated from TOPEX/POSEIDON, launched in 1992.

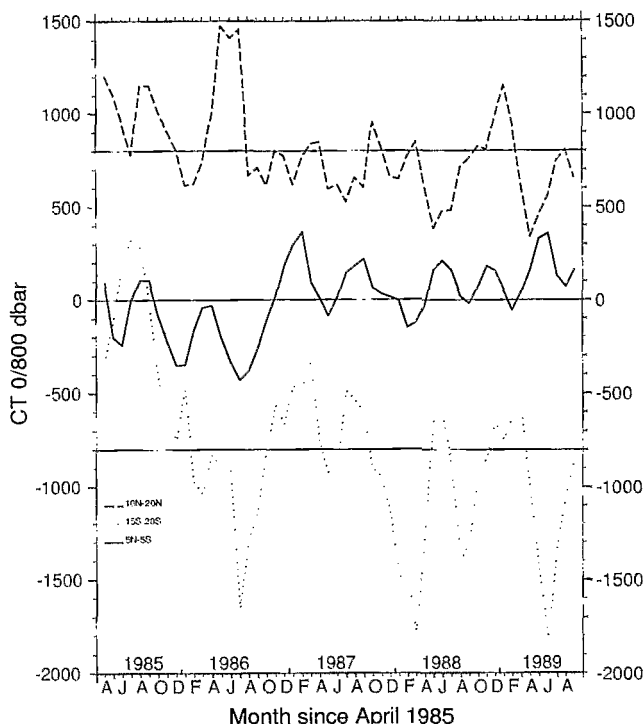


Figure 16. The 0- to 800-dbar heat content interannual anomaly from April 1985 to September 1989 as obtained from XBT merchant ship lines. Three regions have been selected because of their amount of data: 10°–20°N (dashed line), 5°N to 5°S (solid line), and 15°–20°S (dotted line). To clear the picture, the northern region has been shifted by 700 and the southern one by 800. The same exchange between the extra-equatorial regions and the equatorial band is identifiable.

Acknowledgments. The authors wish to thank J. Servain (Université de Bretagne Occidentale, Brest) for giving his wind analysis, as well as A. Morlière and J. Merle (LODYC/ORSTOM, Paris) for the primitive equation model results, J. M. Verstraete (ORSTOM, Paris) for tide gauge data, and J. P. Rebert and A. Dessier (ORSTOM, Brest) for XBT-SSS lines. Interesting discussions with all of these people and with Y. Ménard (CNES, Toulouse) when comparing the results were very helpful to this study. P. Braconnot (LMCE, Saclay) provided useful information about the empirical orthogonal function analysis. This research was funded by the French Institut Français de Recherche Scientifique pour le Développement en Coopération (ORSTOM) and the French Programme National de Teledetection Spatiale. S. Arnault was supported by ORSTOM, and R. Cheney by the NOAA Climate and Global Change Program.

References

- Arnault, S., L. Gourdeau, and Y. Ménard, Comparison of the altimetric signal with in-situ measurements in the tropical Atlantic Ocean, *Deep Sea Res.*, 39(3/4), 481-499, 1992a.
- Arnault, S., A. Morlière, J. Merle, and Y. Ménard, Low-frequency variability of the tropical Atlantic surface topography: Altimetry and model comparison, *J. Geophys. Res.*, 97, 14,259-14,288, 1992b.
- Cane, M. A., and E. S. Sarachik, The response of a linear equatorial ocean to periodic forcing, *J. Mar. Res.*, 39, 651-693, 1981.
- Carton, J. A., and E. J. Katz, Estimates of the zonal slope and seasonal transport of the Atlantic North Equatorial Countercurrent, *J. Geophys. Res.*, 95, 3091-3100, 1990.
- Cheney, R. E., B. C. Douglas, and R. W. Agreen, Geosat altimeter crossover difference handbook, *Manual NOS NGS 6*, 32 pp., Natl. Ocean Serv., Natl. Oceanic and Atmos. Admin., Rockville, Md., 1991a.
- Cheney, R. E., N. S. Doyle, B. C. Douglas, R. W. Agreen, L. Miller, E. L. Timmerman, and D. C. McAdoo, The complete Geosat altimeter GDR handbook, *Manual NOS NGS 7*, 78 pp., Natl. Ocean Serv., Natl. Oceanic and Atmos. Admin., Rockville, Md., 1991b.
- Cheney, R. E., W. J. Emery, B. J. Haines, and F. Wentz, Recent improvements in Geosat altimeter data, *Eos Trans. AGU*, 72, 51, 1991c.
- Delcroix, T., J. Picaut, and G. Eldin, Equatorial Kelvin and Rossby waves evidenced in the Pacific Ocean through Geosat sea level and surface current anomalies, *J. Geophys. Res.*, 96, 3249-3262, 1991.
- Diden, N., and F. Schott, Seasonal variations in the western tropical Atlantic: Surface circulation from Geosat altimetry and WOCE model results, *J. Geophys. Res.*, 97, 3529-3541, 1992.
- Duchêne, C., and C. Frankignoul, Seasonal variations of surface dynamic topography in the tropical Atlantic: Observational uncertainties and model testing, *J. Mar. Res.*, 49, 223-247, 1991.
- Emery, W., G. H. Born, D. Baldwin, and C. Norris, Satellite derived water vapor corrections for Geosat altimetry, *J. Geophys. Res.*, 95, 2953-2964, 1990.
- Garzoli, S. L., Forced oscillations on the equatorial Atlantic basin during the Seasonal Response of the Equatorial Atlantic Program (1983-1984), *J. Geophys. Res.*, 92, 5089-5100, 1987.
- Garzoli, S. L., and E. J. Katz, The forced annual reversal of the Atlantic North Equatorial Countercurrent, *J. Phys. Oceanogr.*, 13, 2082-2090, 1983.
- Haines, B. J., G. H. Born, G. W. Rosborough, J. G. Marsh, and R. G. Williamson, Precise orbit computation for the Geosat exact repeat mission, *J. Geophys. Res.*, 95, 2871-2885, 1990.
- Hisard, P., Observations de réponses de type El Niño dans l'Atlantique tropical oriental Golfe de Guinée, *Oceanol. Acta*, 3, 69-78, 1979.
- Hisard, P., and C. Hénin, Response of the equatorial Atlantic Ocean to the 1983-1984 wind from the Programme Français Océan et Climat dans l'Atlantique Equatorial cruise data set, *J. Geophys. Res.*, 92, 3759-3768, 1987.
- Houghton, R. W., and C. Colin, Thermal structure along 4°W in the Gulf of Guinea during 1983-1984, *J. Geophys. Res.*, 91, 11,727-11,739, 1986.
- Katz, E. J., Equatorial Kelvin waves in the Atlantic, *J. Geophys. Res.*, 92, 1894-1898, 1987.
- Katz, E. J., An interannual study of the Atlantic North Equatorial Countercurrent, *J. Phys. Oceanogr.*, 23, 116-123, 1993.
- Lamb, P. J., Case studies of tropical Atlantic surface circulation pattern during recent sub-Sahara weather anomalies, 1967-1968, *Mon. Weather Rev.*, 106, 282-291, 1978.
- Malarde, J. P., P. De Mey, C. Perigaud, and J. F. Minster, Observation of long equatorial waves in the Pacific Ocean by Seasat altimetry, *J. Phys. Oceanogr.*, 17, 2273-2279, 1987.
- Marsh, J. G., C. J. Koblinski, F. Lerch, S. M. Klosko, J. W. Robbins, R. G. Williamson, and G. B. Patel, The GEM-T2 gravitational model, *J. Geophys. Res.*, 95, 13,129-13,150, 1990.
- Ménard, Y., Observing the seasonal variability in the tropical Atlantic from altimetry, *J. Geophys. Res.*, 93, 13,967-13,978, 1988.
- Merle, J., Seasonal heat budget in the equatorial Atlantic Ocean, *J. Phys. Oceanogr.*, 10, 464-469, 1980.
- Merle, J., Variabilité thermique annuelle et interannuelle de l'océan Atlantique équatorial Est: L'hypothèse d'un El Niño Atlantique, *Oceanol. Acta*, 3, 209-220, 1982.
- Merle, J., and S. Arnault, Seasonal variability of the surface dynamic topography in the tropical Atlantic Ocean, *J. Mar. Res.*, 43, 267-288, 1985.
- Merle, J., M. Fieux, and P. Hisard, Annual signal and interannual anomalies of SST in the eastern equatorial Atlantic Ocean, *Deep Sea Res.*, 26, GATE Suppl. 2-5, 77-102, 1979.
- Miller, L., and R. E. Cheney, Large-scale meridional transport in the tropical Pacific Ocean during the 1986-1987 El Niño from Geosat, *J. Geophys. Res.*, 95, 17,905-17,919, 1990.
- Miller, L., R. E. Cheney, and B. C. Douglas, Geosat altimeter observations of Kelvin waves and the 1986-1987 El Niño, *Science*, 239, 52-54, 1988.
- Millero, J., and A. Poisson, The practical salinity scale 1978 and the international equation of state of sea water 1980, *Rep. 10*, UNESCO, Paris, 1981.
- Morlière, A., P. Delecluse, P. Andrich, and B. Camusat, Evaluation des champs thermiques simulés par un modèle de circulation générale de l'Atlantique tropical, *Oceanol. Acta*, 12, 9-22, 1989.
- Périgaud, C., Sea level oscillations observed with Geosat along the two shear fronts of the Pacific North Equatorial Countercurrent, *J. Geophys. Res.*, 95, 7239-7248, 1990.
- Philander, S. G. H., Variability of the tropical oceans, *Dyn. Atmos. Oceans*, 3, 191-208, 1979.
- Philander, S. G. H., Unusual conditions in the tropical Atlantic Ocean in 1984, *Nature*, 322, 236-238, 1986.
- Philander, S. G. H., and Y. Chao, On the contrast between the seasonal cycles of the equatorial Atlantic and Pacific Oceans, *J. Phys. Oceanogr.*, 21, 1399-1406, 1991.
- Picaut, J., J. Servain, A. J. Busalacchi, and M. Seva, Interannual variability versus seasonal variability in the tropical Atlantic, *Geophys. Res. Lett.*, 11, 787-790, 1984.
- Servain, J., and D. M. Legler, Empirical orthogonal function analysis of tropical Atlantic sea surface temperature and wind stress: 1964-1979, *J. Geophys. Res.*, 91, 14,181-14,191, 1986.
- Servain, J., M. Seva, S. Luckas, and G. Rougier, Climatic atlas of the tropical Atlantic wind stress and sea surface temperature: 1980-1984, *Ocean Air Interact.*, 1, 109-182, 1987.
- Weare, B. C., Empirical orthogonal analysis of Atlantic Ocean surface temperature, *Q. J. R. Meteorol. Soc.*, 103, 467-478, 1977.
- Wyrtki, K., Water displacements in the Pacific and the genesis of El Niño cycles, *J. Geophys. Res.*, 90, 7129-7132, 1985.
- Zimelman, D. F., and A. J. Busalacchi, The wet tropospheric range correction: Product intercomparisons and the simulated effect for the tropical Pacific altimeter retrievals, *J. Geophys. Res.*, 95, 2899-2933, 1990.

S. Arnault, Laboratoire d'Océanographie Dynamique et de Climatologie, Unité Mixte de Recherche 121 Centre National de Recherche Scientifique, Institut Français de Recherche Scientifique pour le Développement en Coopération (ORSTOM), Université Pierre et Marie Curie, UPMC T14-2 case 100, 4 place Jussieu, 75252 Paris Cedex 05, France.

R. E. Cheney, Satellite and Ocean Dynamics Branch, National Oceanic and Atmospheric Administration, Silver Spring, MD 20910.

(Received December 1, 1993; revised May 16, 1994; accepted May 16, 1994.)